Investigation of Part Distortions as a Result of Hybrid Manufacturing

Zicheng Zhu*, Vimal Dhokia, Aydin Nassehi and Stephen T. Newman

Department of Mechanical Engineering, University of Bath, Bath, BA2 7AY, United Kingdom

Abstract

In today's society, the customer driven markets has led to the rapid developments and continuous evolution of manufacturing technologies. The ability to accurately produce complex parts, and to reuse and remanufacture used parts is becoming more prevalent, requiring more efficient and rapid methods to be developed. One such method being currently developed is the hybrid process combining additive, subtractive and inspection processes for the manufacture of complex part geometries from any given raw material in terms of shape and size. A major element of the hybrid process is decomposition of a part into a number of subparts, which are additively manufactured and machined in sequence. However, the residual stresses resulting from the temperature difference between the solidified material (i.e. already manufactured subparts) and the material being deposited (i.e. new subparts being built) leads to part distortions, which significantly reduces the dimensional accuracy of finished parts. This study investigates part distortions that take place in the additive manufacturing process under the context of hybrid manufacturing. A method for conducting this investigation was first proposed. A mathematical model was developed, identifying the influential parameters that contribute to part distortions. These parameters were then incorporated in the experimental design by employing the Taguchi design of experiments strategy. Distortion behaviour arising from thermally induced stress was experimentally explored, indicating that part length, height, and layer thickness have significant effects on part distortions.

Keywords: Part distortion; Hybrid manufacturing process; Fused filament fabrication; Additive manufacturing

1 Introduction

The 21st century demand for innovation is leading towards a revolution in the way products are perceived [1]. However, due to the technological constraints of individual manufacturing processes, it is not always feasible to produce components in terms of material, geometry, tolerance and strength etc. [2, 3]. Additive manufacturing (AM) techniques, as one of the representatives of the new manufacturing methods, provide the capability with which to produce complex geometries, for

* Corresponding author, e-mail address: Zicheng.Zhu@bath.edu

example, internal features, which are virtually impossible to create with any other manufacturing process. Nevertheless, surface quality and accuracy impedes its further development for producing end user products with high accuracy [4]. Computer Numerical Control (CNC) machining, on the other hand, provides the capability to generate components with extremely high levels of accuracy and surface finish, but it is still relatively difficult to machine certain complex geometries and shapes owing to tool inaccessibility problems [5, 6]. As a result, hybrid processes, which combine different processes together, have drawn significant attention due to their ability to capitalise on the advantages of independent processes whilst minimising their disadvantages [7].

A typical configuration of the hybrid processes is the combination of additive and subtractive processes [3]. Integrating CNC machining with AM processes may provide new solutions to the limitations of additive processes [8] due to the high accuracy, improved quality and speed that machining processes offer. In addition, the capability of the AM processes in producing complex part geometries can be utilised. Jeng and Lin [9] used a laser to melt the mixed powders (Fe, Ni and Cr). Once one cladding operation was accomplished, the surface of the cladding was milled in order to achieve the desired accuracy and maintain a flat surface for the next cladding operation, until the entire mould was produced. Song and Park [10] utilised two gas metal arc welding guns for deposition of different materials, and CNC milling to finish machine the deposited injection moulds. Karunakaran *et al.* [11] used face milling to machine each slice built by metal inert gas and metal active gas welding. Ruan *et al*. [8] and Ren *et al*. [12] incorporated a laser cladding unit with a five-axis milling machine, where any deposition feature can be built in the horizontal direction by rotating the workstation. However, one of the major problems of these hybrid processes is the rapid contraction of the material after it is deposited. The new material is deposited onto the part that has previously been built or machined. The contraction of the newly deposited material can induce residual stresses and distort the final product shape, significantly reducing the part accuracy. An example can be found in Figure 1, where the new material (blue part) was built on the white part that had been previously made. The heat was dissipated during deposition of the blue part. As a result, the rapid temperature reduction after the blue material was extruded caused the material to quickly solidify and contract, which consequently pulled up the white part.

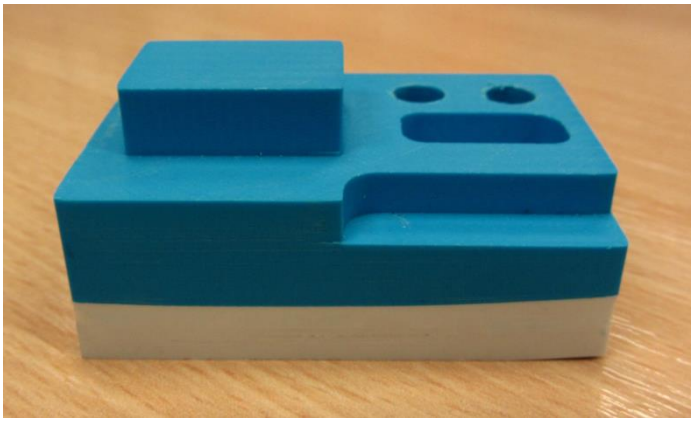

Figure 1 – Part distortions in continuously depositing new material

Therefore, this study is aimed at investigating the distortion behaviour in the additive process under the context of hybrid manufacturing. The related research on part distortions in individual additive processes was first reviewed in section 2. A novel concept of the hybrid process consisting of additive, subtractive and inspection processes was proposed. The part distortion behaviour in this specific hybrid process was then investigated. A mathematical model was developed, which was used to select process parameters in the design of experiments (DoE) stage. The experiments were conducted and finally the results were statistically analysed, identifying the relationship between the distortion behaviour and the process parameters.

2 Review of the related work on part distortions

Although there is no research reported on part distortions for hybrid processes, a number of efforts have been made on the investigation of the effects resulting from various process parameters in relation to part distortions for individual additive processes.

Nickel *et al*. [13] examined the effect of deposition patterns on the resulting stresses and deflections in the Shape Deposition Manufacturing (SDM) process. Both finite element analysis and experiments show that the deposition pattern has a significant impact on the deflection of the manufactured part. The interaction between the process parameters and material properties also influence the deflection. Material properties such as dynamics of polymerisation related to the amount of volume shrinkage in the Stereolithography (SLA) process was investigated by Wiedemann *et al*. [14]. They further identified that the dynamics of polymerisation can be used to optimise hatching strategies for reducing internal stress, which in turn diminishes the curl development of the part surface. Dalgarno [15] carried out a structural analysis, modelling the curl development of the parts in the Selective Laser Sintering (SLS) process. Double sintering the first two layers was found to be an effective way to reduce the curling level. Sonmez and Hahn [16] developed a thermo-mechanical model investigating temperature and stress distributions in each layer in the laminated object manufacturing process. A

large roller diameter and slow roller speed are recognised as beneficial for laminate bonding, and it is suggested that these two factors could contribute to part warpage. Zhang and Faghri [17] developed a physical model where melting a mixture of two powders with significant different melting points was explored. It was found that the porosity of the part contributes to the shrinkage, leading to distortions. The shrinkage phenomenon accelerates the melting process while the material is at fixed solid phase. Chin [18] studied the thermo-mechanical relationship between droplet columns and adjacent droplets in the SDM process. The established model shows that the process-induced pre-heating has noticeable impact on the reduction in thermal gradients and residual stresses, which consequently reduces distortions. Xu *et al*. [19] studied the distortion deformation of the plate parts and developed a mechanical equivalent model of resin phase change shrinkage in the SLA process. Yang *et al*. [20] developed a scale factor in three dimensions to compensate the distortions of the SLS components caused by the material phase changes during the laser sintering process. The Taguchi method was applied to maintaining dimensional accuracy against the changes in the build positions and part size. The accuracy was improved by up to 24% compared with the counterparts made by other commercial machines.

A number of research activities have been carried out, identifying the effects caused by the deposition patterns. The raster pattern with lines oriented 90° from the long axis of the rectangular block produces the lowest deflections [13]. Klingbeil *et al*. [21] identified that when depositing in a raster path, material should not be deposited parallel to the longest part dimension. This is because the curvature is the greatest parallel to the deposition direction and depositing parallel to the longest part dimension would result in greater warping deflections and loss of tolerance. The raster pattern with lines 45° and concentric pattern generate low and uniform deflection but the part produced by using the former pattern shows better mechanical property in terms of stiffness and bonding strength between adjacent layers [22]. The deflection and mechanical properties of the part by using Hilbert curve and Octagram spiral remain undeveloped. An initial study has been conducted, showing Hilbert curve and Concentric patterns generate smaller substrate deflections, compared with raster 0° [23].

Wang *et al*. [24] simplified the factors that affect the part deformation phenomenon and therefore proposed a mathematical model where only temperature, length of cross-section and layer thickness were considered. By theoretically analysing the model, linear and non-linear relations between these factors have been obtained, indicating that the changes of each factor significantly influences the part accuracy. Zhang and Chou [25] developed a comprehensive finite element model, which is able to simulate the Fused Deposition Modelling (FDM) process involving mechanical and thermal processes. Experiments were also conducted and the results were compared with the simulation results, revealing that scan speed is the most significant factor followed by the layer thickness. In slicing Computer Aided Design (CAD) models, the inconsistent layer geometry containment where all the approximated extruded square-edged layers do not correspond to the minimum circumscribed volume

results in systematic distortion [26]. Chen and Feng [26] proposed a layer contour generation approach, creating the minimum circumscribed extruded layered geometries. Along with the developed marching algorithm, which generates the boundary contour for each layer, the systematic distortion in AM parts can be eliminated. Yu *et al*. [23] explored part distortions, interior quality and mechanical properties of the laser solid forming manufactured parts by using four deposition tool path patterns, namely raster, offsetin (offset from the inside to the outside), offsetout (offset from the outside to the inside) and fractal. Both finite element analysis and experiments show that the part distortions are primarily influenced by the transient temperature gradient arising from deposition patterns. The smallest deformation was obtained when using fractal pattern followed by offsetout. Vatani *et al*. [27] employed the classical lamination theory to model mechanical properties of layers, layer shrinkage and residual stress growth during the SLA process by taking into consideration the heterogeneous property of the SLA parts. The model was then used to predict the curvature of distorted parts, identifying that increasing layer thickness results in decreased degree of distortion. It was also found that the distortion degree is proportional to part height.

3 A novel concept of hybrid manufacturing process

3.1 The hybrid process – iAtractive

The concept of the hybrid process (entitled iAtractive) consists of combining additive (fused filament fabrication, FFF[†]), subtractive (CNC machining) and inspection processes [28, 29]. This is based on the need to reuse and remanufacture existing parts or even recycled and legacy parts; enhance the flexibility of CNC machining and improve the accuracy of FFF process [30]. Incorporating an additive process releases design constraints often caused by tool accessibility issues in CNC machining. Using CNC machining capabilities the final part can be produced with a high degree of accuracy comparable to that of an entirely CNC machined part. Furthermore, dimensional information of the existing part can be obtained by using an inspection technique enabling the existing part to be further manufactured by an additive and/or subtractive process, providing new enhanced functionalities [31].

3.2 Part distortions in the iAtractive process production

In order to investigate part distortion behaviour, it is important to understand the basic working principle of the iAtractive process and how distortion takes place. An example scenario of the iAtractive process production is to add the material using the FFF process followed by a machining operation. More material is then added onto the machined part which is further subject to machining and inspection operations until the final part is produced, as shown in Figure 2. It should be noted that

[†] Fused Filament Fabrication (FFF) is sometimes called Fused Deposition Modelling (FDM). However, the latter term is trademarked by Stratasys Inc., and cannot used publicly without authorisation from Stratasys Inc.

this study is focused on the experimental investigation of part distortions that take place in the FFF process under the context of the iAtractive process production.

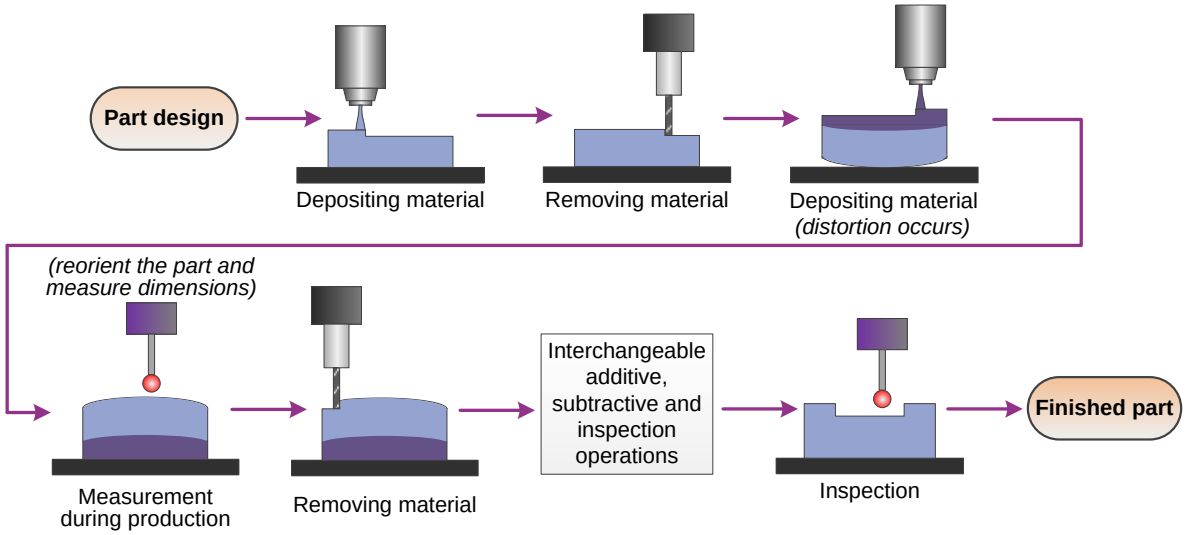

Figure 2 – An example scenario for part production using the iAtractive process

Due to temperature gradients involved in the FFF deposition process, thermal stresses develop [13]. These stresses arise from the contraction associated with the deposition of each layer, resulting in distortions or even failure of the deposition process. The previously deposited, machined part, existing part or legacy product (for convenience, all of them are seen as existing parts) is considered as being in a room temperature state (20ºC). This is because warming it up to the glass transition temperature (T_g = 60ºC) is highly time consuming, which significantly increases the production time. More importantly, even though the existing part has been placed and heated on the heated bed of the FFF machine, it is highly unlikely that the heat can be equally distributed in the entire existing part, achieving a constant temperature due to thermal conduction as well as the part geometry. Moreover, once the existing part has been heated, the temperature difference between its bottom and top leads to part distortion behaviour being even more complicated to quantify. As a new additive operation starts, bonding between the newly deposited layer and the previous layer takes place by local re-melting of previously solidified material and diffusion [32]. The heating and rapid cooling cycles of the material lead to non-uniform thermal gradients that cause continuous stresses accumulation, resulting in further distortions between the existing part and the part built upon it. The distortion behaviour can be found in Figure 1 as an example, which is similar to the example depicted in Figure 2 (the step called ‘depositing material, distortion occurs’). In this case, the bottom surface has to be finish machined.

4 The method for investigating part distortion behaviour in the hybrid process production

Due to each additive process involving a large number of process parameters, the change of any parameter may lead to the quality changes of the final part. It is impractical to explore the effects

caused by every FFF process parameter. From the literature survey reported in section 2, it can be identified that there is no consensus on which process parameters are of the most significance in terms of part distortions. The process parameters that govern the warp deformation behaviour could be completely different depending on each individual additive process. To the author's knowledge, there is no research on part distortions of FFF processed parts.

In order to explore the distortion behaviour in the iAtractive process, the parameters to be investigated in the experiments need to be determined. A simplified mathematical model was thus first developed, identifying the primary influential process parameters. These parameters were analysed and four parameters were then selected. The test parts were designed based on the four selected parameters. The Taguchi DoE strategy was adopted for designing a series of experiments. The analysis of variance (ANOVA) technique was used to analyse the results, identifying the most significant parameters that lead to part distortion. This method is represented in the following IDEF0 representation in Figure 3.

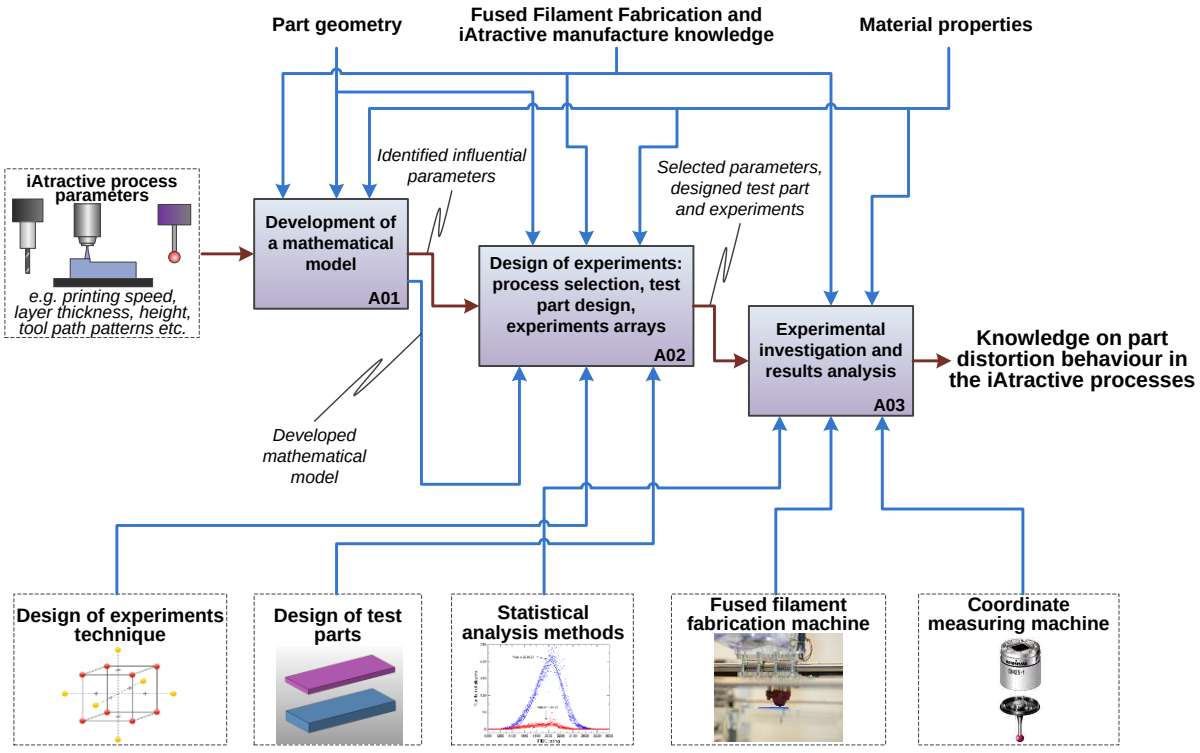

Figure 3 – The method for investigating part distortion behaviour

5 The simplified mathematical model of distortion deflection

As this study is focused on the experimental investigation of distortion, the parameters to be investigated should be selected in the DoE stage. Thus, a mathematical model was developed, which only aimed to identify the possible major factors that may affect the part distortion behaviour. These

factors were then involved in the DoE stage. It should be noted that this mathematical model is not developed to accurately predict the distortion behaviour.

5.1 Assumptions

The following assumptions are made, which simplifies the FFF process and allows the mathematical model to focus on the major factors that are influential to distortion.

- Deposition speed is constant. The constant and steady deposition speed means the stress inside each deposited fibre of the layer plane can be considered as uniform.
- The deposited part does not have voids. The existence of voids between stacking fibres implies the structure changes in micro areas, which means the stresses do not change uniformly and continuously.
- Residual stresses in each layer do not accumulate when the temperature decreases from the melting temperature (T_m) to T_g. As an amorphous plastic, PLA can no longer withstand much stress at temperatures above its T_g, in which case, significant deformation may occur. In other words, in spite of the fact that the part is subjected to contraction due to the temperature difference between T_m to T_g, no residual stress accumulates. The residual stress is largely induced by the cooling process between T_g to room temperature (T_r), which results in part distortions.
- The existing part or the part directly built on the heated bed is considered to be unwarped.
- Each layer is produced and completed instantaneously in this mathematical model. Research has reported that it takes approximately 0.55s to reach the material T_g (94°C) once the material (i.e. Acrylonitrile Butadiene Styrene, ABS) is extruded from the nozzle (T_m = 270°C) and only 1.2s is needed from T_g to the FDM machine chamber temperature (70°C) [33]. Although no research data have been published for PLA whose both T_m (195°C) and T_g (55°C) are much lower than that of ABS, it is obvious that the cooling time for PLA can be regarded as infinitely small compared to the build time for fabricating a middle-sized prototype cube (e.g. 50×50×50 mm^3). In this case, for simplifying the mathematical model, the part is considered as being stacked by a number of layers and each layer is finished instantaneously.

5.2 A simplified mathematical model

Given that the process plan for manufacturing a part using the iAtractive process is generated based on the part design, features and the dimensions are the most accessible geometrical information for the iAtractive process [28, 30]. The mathematical model is thus focused on part dimensions that affect the degree of distortions, and the material properties that essentially cause distortions. Figure 4 depicts a scenario before distortions take place, where a layer (thickness of t) with length of L_s is deposited onto an existing part with L_s in length and h_e in height.

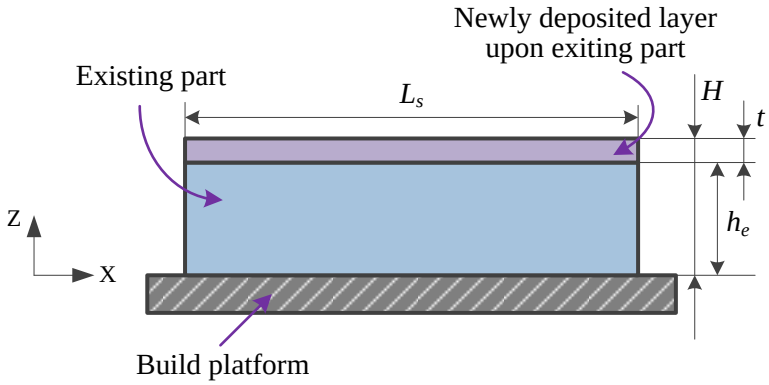

Figure 4 – Deposition of a new layer onto an existing part

While distortions occur during the material cooling and deformation finally and completely forms (as shown in Figure 5), the main body of the entire part achieves equilibrium. This means the net force between thermal induced stress (σ), the bending stress (τ) and a constant stress (σ_c) has to be zero [24], which is depicted in Equation 1 below.

Equation 1:
$$\int_0^{h_e+t} (-E\alpha(T_g - T_r) + \kappa E(z-\gamma)) \cdot dz = 0$$

where, E is Young's modulus of elasticity, α is coefficient of thermal expansion and γ is the distance between the position of the neutral axis and the surface where the nozzle moves, κ is the curvature.

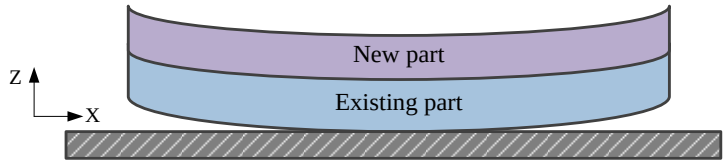

Figure 5 – Part distortions occur while adding material to an existing part

In addition, the net moments generated by these forces (σ, τ and σ_c) are equal to zero [24], see Equation 2.

Equation 2:
$$\int_0^{h_e+t} [-E\alpha(T_g - T_r) + \kappa E(z-\gamma)] \cdot z \cdot dz = 0$$

Solving trigonometric function relationships and simply slicing the part into layers, the distortion displacement (s) for depositing n new layers can be obtained, using Equation 3.

Equation 3:
$$s = \frac{(N+n)^3 t}{6\alpha N(T_g - T_r)} \times \left[1 - \cos\left[\frac{3\alpha N L_s}{(N+n)^3 t}(T_g - T_r)\right]\right]$$

where, N is the number of layers for the existing part, and n is the number of layers deposited onto the existing part. From Equation 3, it can be identified that, in the scenario specified in the above assumptions, the degree of distortion described by the distortion displacement (s) depends on the

height of the existing part, the number of layers to be deposited onto the existing part, and the section length of the existing part and the newly deposited part. This finding is used to design the experiments in the proceeding subsection.

6 Design of Experiments

6.1 Determination of process parameters

According to the literature review in section 2 and the mathematical model in section 5, the influential factors are discussed as follows:

- *Deposition speed/nozzle travelling speed*: the main effect resulting from the changes of travelling speed is the frequency changes of the material heating and cooling cycle, which essentially alters the degrees of thermal gradients, affecting the thermal-induced stresses accordingly. However, the nozzle travelling speed is considered to be constant during the entire iAtractive process and the effect caused by deposition speed will be discussed in section 7.
- *Layer thickness (t)*: it directly determines the number of layers to be deposited for printing a part. Fewer layers indicate a lesser number of material heating and cooling cycles and vice versa. The influence on part distortions as a result of using different layer thicknesses is investigated in section 7.
- *Part porosity/density and extrusion infill width*: increased part density requires more material to fill in certain areas in each layer, increasing the length of the tool path. As a result, more heat is introduced. By contrast, increasing extrusion infill width can effectively reduce the number of loops required for printing a layer, which consequently reduces the tool path length as well as heating and cooling cycles. However, wider infill width will also increase more heat input within a certain period of time, which can result in more obvious distortions during material cooling. Additionally, voids between rasters of two adjacent layers also affect heat dissipation and thus may decrease residual stresses. Hence, for maximising distortion behaviour, 100% density was used in the experiments.
- *Deposition pattern*: the effects of using different deposition patterns have been explored, as reported in section 2. Given that the purpose of this study was to investigate the distortion behaviour when adding new material onto the existing parts in the iAtractive process, the raster 45^{o} pattern was chosen for the experimentation, which is also the most widely used pattern in FFF [22].
- *Part geometry*: distortion is also geometry dependent, which is virtually impossible to quantify. A typical example is given in Figure 6, which is the top view of the cross-section of the parts. The part distortion in Figure 6(a) is relatively easier to predict, if all the above mentioned parameters are constant. However, the part distortion in Figure 6(b) is far more complicated since

this relates to the deposition patterns. Using the raster 45° pattern, for example, the shape edge highlighted in the red circle can have (i) long continuous tool path; or (ii) short continuous tool path (see Figure 7, in which white lines are tool paths), depending on the position of the shape edge. As discussed above, long tool paths are likely to produce greater degrees of deflection. In addition, the tool path also varies while changing the magnitude of angle θ, leading to the variation of the residual stress distributions. Furthermore, the build direction of the existing part may be different from that of the new part being built upon the existing part, which means the deposition patterns of these two parts are possibly different. For simplifying the experimental design, a rectangular block is adopted as the part geometry in the experiments, which will be introduced in section 6.2.

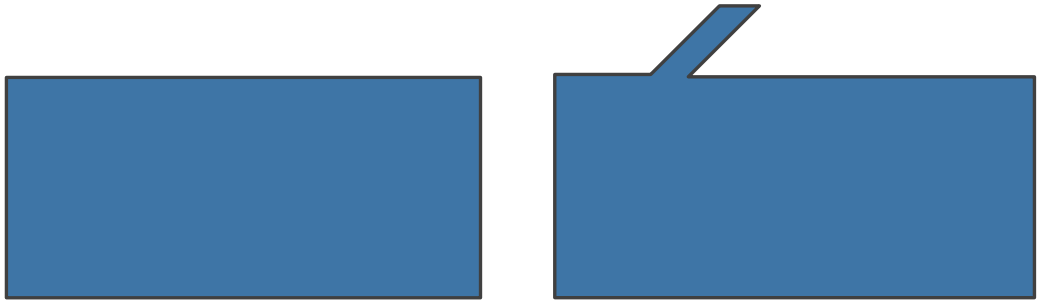

(a) (b)

Figure 6 – The difference resulted from two part geometries in part distortions

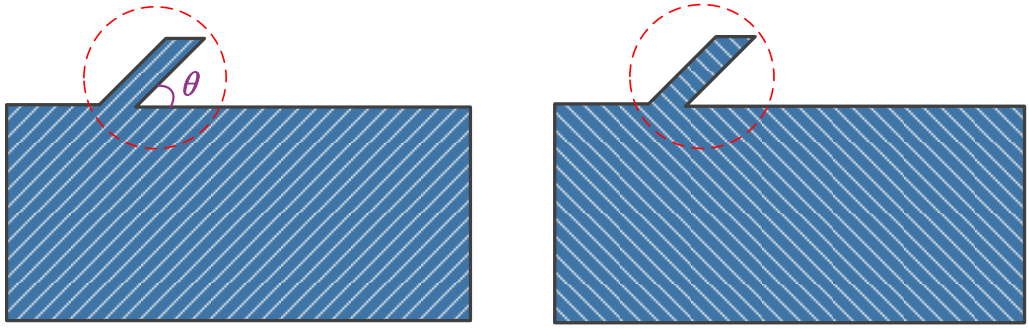

(i) (ii)

Figure 7 – The tool paths for printing part (b) in Figure 6

- *Section length of the existing part (L_s), heights of the existing part (h_e) and the newly deposited part (h_n)*: these three parameters have already been identified as important parameters (in Equation 3) that have direct effects on part distortions. These three parameters are also the most accessible geometrical information to be used to generate process plans for the iAtractive process [30].

To this end, the influential parameters to be investigated together with the other parameters to be used in the experiments have been defined. It is worth mentioning that all of the above parameters are interrelated. Given the purpose of the part distortion investigation, L_s, h_e and h_n and t were selected.

6.2 Design of test parts

Two rectangular blocks were designed, as shown in Figure 8. Part A is an existing part and part B is deposited directly onto the top of part A.

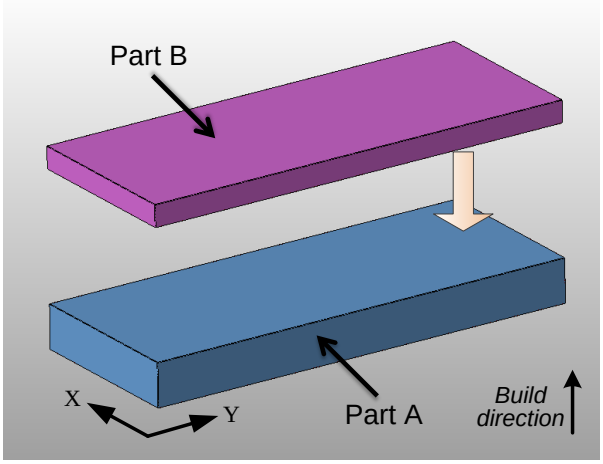

Figure 8 – Test part design for the investigation of part distortion

6.3 Taguchi design of experiments

The Taguchi DoE strategy was used and three levels were applied to each parameter, representing low, medium and high levels, respectively. By considering the working volume of the FFF machine, 60mm, 90mm and 120mm were chosen for section length (L_s). Producing a block of 100cm^3 would cost significant increase in build times, thus 3mm, 6mm and 9mm were decided to be the three levels for the heights of the existing parts (h_e). These three levels of h_e were also applied to the heights of the newly deposited parts (h_n). By doing so, the ratio of h_e to h_n can be 33%, 50%, 67%, 100%, 150%, 200%, 300%, which covers a wide range of the scenarios where the new part is added onto the existing part. The layer thicknesses of 0.2, 0.25 and 0.3mm were used, which are the most stable set up used for the FFF machine. The interactions between L_s, h_e and h_n were also taken into consideration. Therefore, an L27 Taguchi orthogonal array was generated. The variables and the other process parameters to be used in the experiments are listed in Table 1.

Table 1 – Process parameters used in the part distortions experiments

Process parameter	**Level**			**Unit**	**Definition**
	1	2	3		
Section length (L_s)	60	90	120	mm	See Figure 4
Height of existing part (h_e)	3	6	9	mm	See Figure 4
Height of newly deposited part (h_n)	3	6	9	mm	See Figure 4
Layer thickness (t)	0.2	0.25	0.3	mm	See Figure 4
Fixed factors	**Value**			**Unit**	**Definition**
Extrusion temperature	205			°C	The operating temperature of the nozzle/extruder
Deposition nozzle speed	2500			mm/min	The speed at which the deposition nozzle travels
Deposition pattern	45° raster			N/A	See Figure 7
Road width	0.5			mm	The width of deposition line
Perimeter to raster air gap	0.0			mm	The distance between the perimeter and raster infill
Part density	100			%	The porosity of the part
Infill overlap	0.2			mm	The distance the infill overlaps with the outline perimeter

7 Results and discussion

The top surface of each newly deposited part (Part B in Figure 8) was face milled with 0.5mm removed in order to achieve a flat surface as a datum for measurement. The bottom surface of each test part (in reference to the build direction) was measured using the scanning mode on a coordinate measuring machine, as showed in Figure 9. The white part is the existing part (i.e. part A) and the blue part is the newly deposited part (i.e. part B). The part was positioned in the direction opposite to the build direction. A large number of 0.5mm equally spaced points were collected for each scanned line along the section length (Y axis). In order to obtain the results as accurately as possible, 5 lines with 4mm interval between each other along the X axis were scanned. The measurement results are listed in Table 2 together with the Taguchi DoE array output.

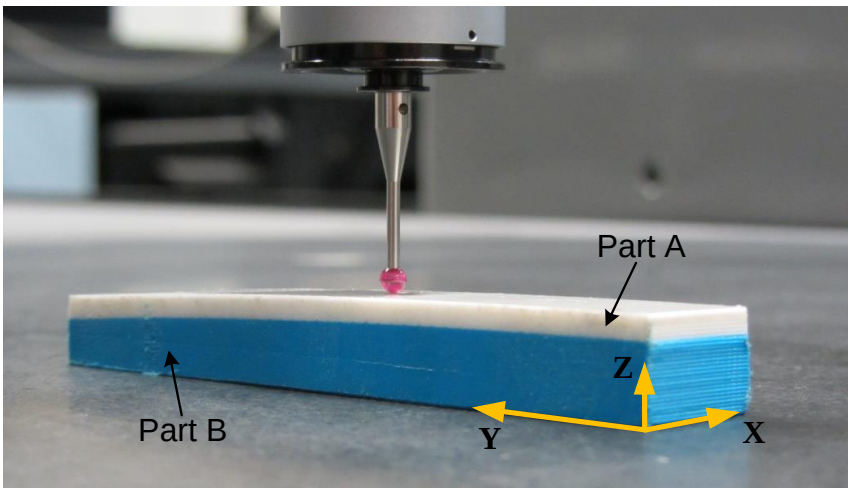

Figure 9 – Scanning the bottom surface of a test part

Table 2 – Experimental runs and measurement results for part distortion analysis

Experimental run	Factor and level				Distortion displacement (mm)
	Section length L_s	Height of existing part h_e	Height of new part h_n	Layer thickness t	
1	1	1	1	1	0.465
2	1	1	2	2	0.380
3	1	1	3	3	0.521
4	1	2	1	2	0.192
5	1	2	2	3	0.267
6	1	2	3	1	0.155
7	1	3	1	3	0.190
8	1	3	2	1	0.066
9	1	3	3	2	0.166
10	2	1	1	2	0.714
11	2	1	2	3	0.710
12	2	1	3	1	1.285
13	2	2	1	3	0.278
14	2	2	2	1	0.314
15	2	2	3	2	0.186
16	2	3	1	1	0.316
17	2	3	2	2	0.364
18	2	3	3	3	0.389
19	3	1	1	3	1.158
20	3	1	2	1	1.438
21	3	1	3	2	1.263
22	3	2	1	1	0.250
23	3	2	2	2	0.487
24	3	2	3	3	0.720
25	3	3	1	2	0.086
26	3	3	2	3	0.426
27	3	3	3	1	0.285

(1: low, 2: medium, 3: height)

The ANOVA approach was used to statistically analyse the results, identifying significant parameters and interactions between these parameters. The analysed results are shown in Table 3, indicating that

the height of the existing part is the most significant parameter, followed by the section length. The height of newly deposited part and the layer thickness are insignificant. It was found that the layer thickness of 0.25mm produces the smallest degree of distortion as compared to the layer thickness of 0.2mm and 0.3mm, as demonstrated in Figure 10. The three points shown in each plot of the four control factors represent the mean of the measured distortion deviation while such a factor was set at different levels (i.e. from low to high), respectively. The plots illustrate that while applying low section length and/or high value of existing part height, the degree of distortion deviation is significantly lower than that of other factors' levels. Unlike the assumptions proposed in the DoE and the analysis in the mathematical model, layer thickness and height of newly deposited part do not contribute to the majority of the changes in distortion deviation. Regarding the parameter interactions, the interaction of section length and height of the existing part is of primary significance. Therefore, the top three greatest tolerance losses were observed in the test parts, of which L_s was 120mm and h_e was 3mm. In addition, the top three smallest degree of warp deformation were found in the test parts, where L_s was 60mm and h_e was 9mm.

Table 3 – ANOVA table for the analysis of part distortions

Source	**DOF**	**Sum of squares (*SS*)**	**Adj Mean square (*MS*)**	**F**	**P**
Section length (*A*)	2	0.77	0.39	19.80	0.01
Height of existing part (*B*)	2	2.15	1.07	55.18	<0.001
Height of newly deposited part (*C*)	2	0.10	0.05	2.53	0.16
Layer thickness (*D*)	2	0.025	0.01	0.63	0.56
*A*B*	4	0.47	0.12	6.03	0.03
*A*C*	4	0.11	0.03	1.46	0.32
*A*D*	4	0.11	0.03	1.42	0.33
Error	6	0.12	0.02		
Total	26	3.86			

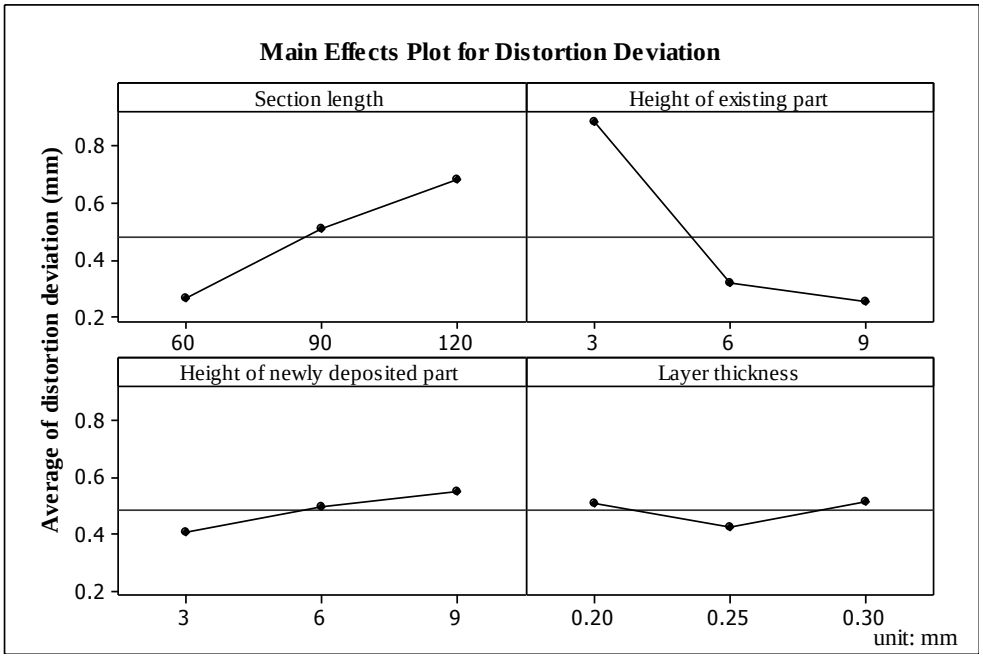

Figure 10 – The main effect plot for part distortions

Figure 11 shows the significance of interaction between two factors. From blocks L1_C2, L3_C2 and L4_C2, it can be identified that increasing the height of the existing part can significantly reduce the distortion deviation. The blocks L2_C1, L3_C1 and L4_C1 reveal that increasing section length leads to increased degree of distortion. However, the change of layer thickness or height of newly deposited part does not have significant influence on part distortion, as identified in block L3_C1 and L4_C1. In terms of the interaction between the height of existing part and other three factors (blocks L2_C1, L2_C3 and L2_C4), the height of the existing part is far more important than the other three factors, which supports the ANOVA results presented in Table 3. Table 3 also identifies that the height of newly deposited part and layer thickness are insignificant factors. As a result, their interaction is insignificant as well, as shown in block L3_C4 and L4_C3 where the distortion deviation does not fluctuate severely while changing either of the factors.

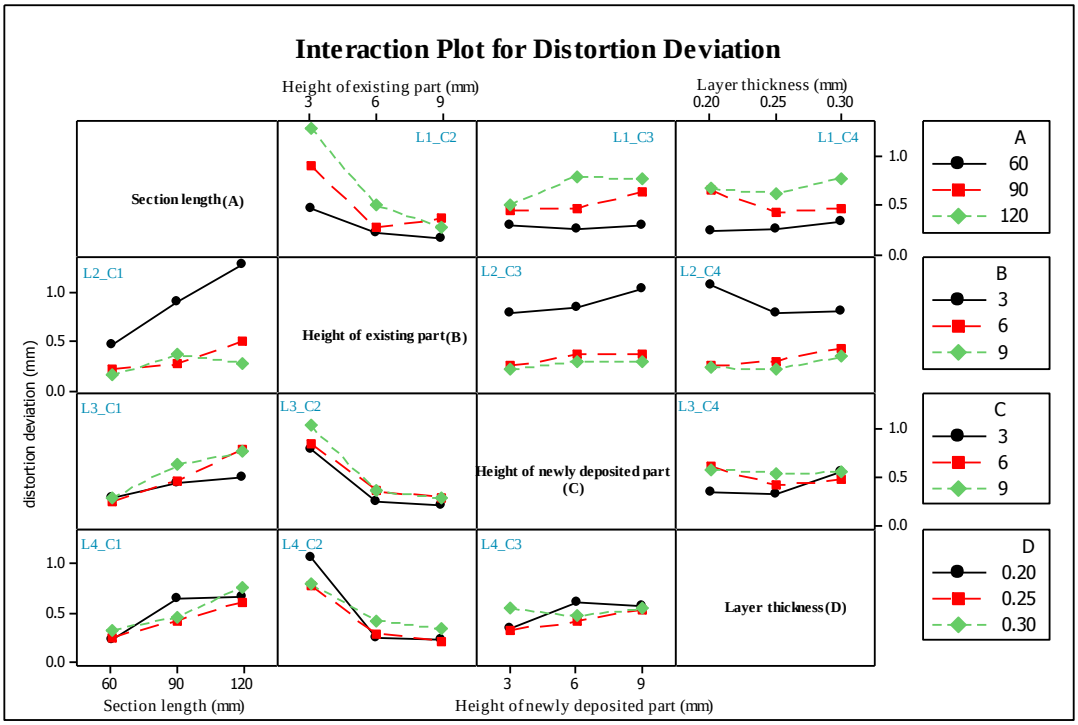

Figure 11 – Interaction plot for distortion deviation

The residual stresses are the main reason that results in L_s, h_e and their interaction being significant. Shrinkage along the deposition tool path may be attributed to the development of residual stresses resulting from the contraction of deposited thermoplastic fibres. The contraction is caused by the rapid cooling of the deposited material from its extrusion temperature (205ºC) to T_g (60ºC) in a very short period of time. However, it should be noted that, at this temperature range the deposited fibre can acquire a large deformation with less force and the capacity to resist outside force is small [34]. As a result, despite contraction, residual stresses are not accumulated in this temperature range. Nevertheless, when cooling from T_g to T_i (20ºC), stress (σ) given by Equation 4 is developed and continuously accumulated.

Equation 4 $$\sigma = -E\alpha \cdot (T_g - T_i)$$

Equation 5 $$dl = (T_g - T_i) \cdot \alpha \cdot L_0$$

where, E is Young's modulus of elasticity, dl is the change in length (unit: mm), T_g is the glass transition temperature (°C), T_i is the inspection room temperature, α is the coefficient of linear thermal expansion and L_0 is the initial length.

Moreover, in the FFF process, heating and rapid cooling cycles of the material results in non-uniform temperature gradients [24]. Consequently, this leads to build up in stresses, which further causes distortions, resulting in dimensional inaccuracy and inner layer cracking or even delamination. The reason attributed to non-uniform heating and cooling cycles is the working principle of the FFF process. That is heat dissipated by conduction and convection during the entire deposition process.

The rapid reduction in temperature enables the material to quickly solidify onto the surrounding filaments [34]. The heat brought from the newly deposited material diffuses to the previously solidified material, generating local re-melting effects, realising strong bonding between the filaments and adjacent layers.

This leads to uneven heating and cooling of material and in turn, generates non-uniform temperature gradients. As a result, uniform stress will not be developed in either the newly deposited part or the existing part. The existing part can no longer regain its original dimension completely. Furthermore, higher stresses are found along the long axis of the deposition tool path [21]. In addition, according to Equation 5, the longer the part, the greater the linear contraction. As a result, the longer section length directly leads to greater tolerance loss.

The scanned points were used to plot the contour of the bottom surface of each test part. The contour of the bottom of test part 19 is displayed in Figure 12 (L_s = 120mm, h_e = 3mm, h_n = 3mm, t = 0.3mm). However, it should be noted that the profile has been displayed in an inverted configuration. This vaulting shape is the typical distortion pattern and all the measured test parts show the similar pattern. It was found that the distortion core shifts away from the geometric centre of the bottom surface along the Y axis. This phenomenon can be explained using the conclusion obtained from the simulation results by Zhang and Chou [25], who identified that the developed asymmetric stress is distributed during the deposition process. As a result, the position of the distortion centre is shifted. Yu *et al.*'s [23] results derived from the finite element analysis of temperature distributions also support this finding, demonstrating that the highest temperature zone is not located in the centre of the cross-section of the part in the XY plane.

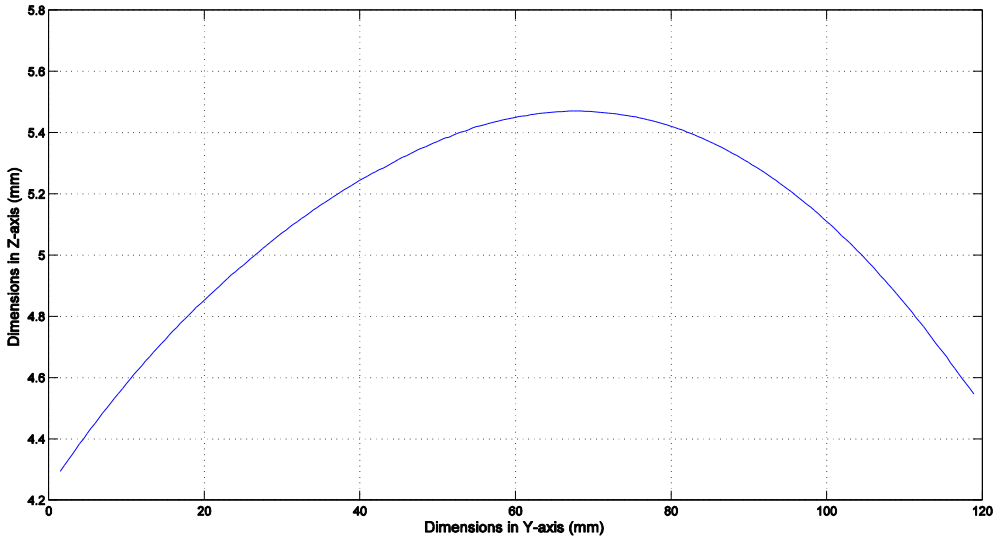

(a) Two dimensional profile

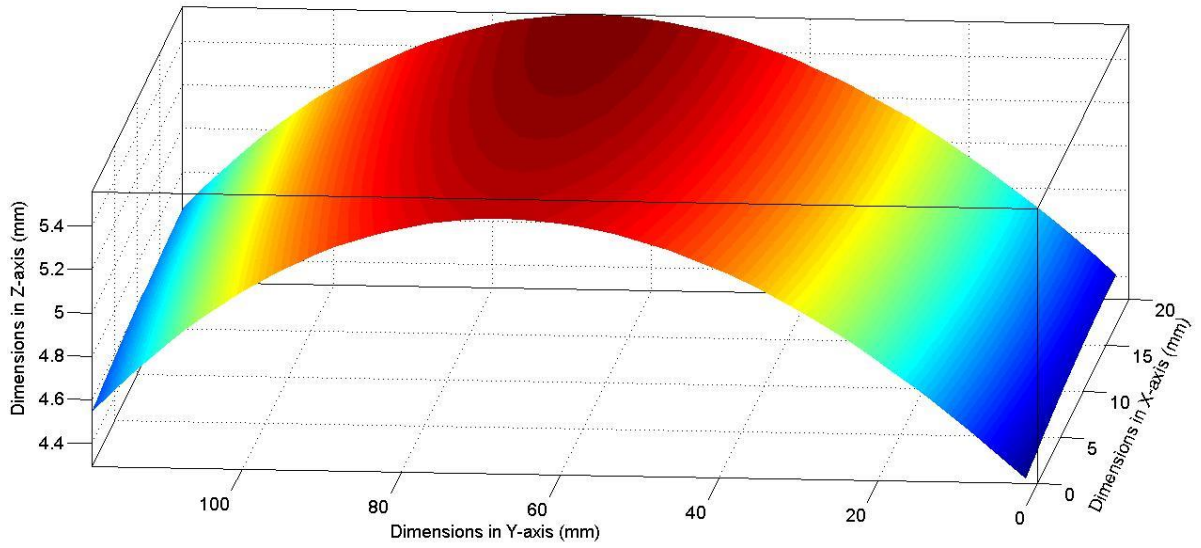

(b) Three dimensional profile

Figure 12 – The curvature formed at the bottom of test part 19

There are also other factors that lead to non-uniform heating and cooling cycles:

- Extrusion speed. This is the speed at which the nozzle is extruding the material. Extrusion speed may alter the heating and cooling cycle and result in different degree of thermal gradient. Thus, it also affects the part distortions and dimensional accuracy [25]. Obviously, at lower slice thickness (e.g. 0.2mm), the extrusion speed is slower as compared to higher slice thickness (e.g. 0.3mm). This is because, in the same per unit length and the same unit time, more material has to be extruded when printing a 0.3mm depth layer than that of a 0.2mm depth layer.

- Deposition speed/nozzle travelling speed. As introduced in the experimental design (section 6.1), the changes of deposition speed also results in non-uniform heating and cooling. Moreover, the nozzle travelling speed has to significantly decrease when the nozzle is approaching a corner on a continuous tool path or depositing material at the turns near a part boundary. After passing through the turn/corner, the nozzle accelerates until it achieves the constant speed (i.e. the speed at which the nozzle prints a straight line). If the length of a tool path is short, this will require accelerating and decelerating the nozzle travelling speed in a short period of time, leading to non-uniform stress build up, particularly near the part boundary.

- Deposition patterns. As described in the DoE, the pattern used to deposit material has an effect on the heating and cooling cycle and furthermore the resulting stresses and part deformation. According to Equation 5, higher stresses are usually found along the long axis of a deposition line, as shown in Figure 7(i). This also explains the reason that the degree of part distortions is

smaller in Hilbert curve than that of raster 0º in Yu *et al.*'s [23] work. Thus, it is advisable to adopt short raster lengths along the long axis of part to reduce the stresses.

In addition, further distortion may develop in the circumstances where the new material is added onto the existing part and then subject to machining operations, as shown in Figure 2 (removing material). Typically, material response has two facets, namely, distortion and residual stresses. If the part has a higher resistance against distortion, the residual stresses will increase. When a part of the material is removed, the static equilibrium is upset and stress distribution is altered. Some residual stresses may be relieved, which leads to additional distortions depending on the heights of the newly deposited part (h_n) and the existing part (h_e). If the newly deposited part is high/thick enough, it will be able to provide high resistance against residual stresses and thus, no obvious distortion will occur after the bottom surface of the part is machined off. However, if both the existing and newly deposited parts are very thin, machining a few layers off is highly likely to induce additional distortion. The removal of the surface layer generates a moment in the cross section. In order to balance this moment, the remaining part bends to some curvature and this curvature varies according to the thickness of the material removed. Further investigation is needed to identify the relationships between residual stresses, h_n, h_e and machining parameters. Measurement techniques, such as the layer-removal [35] and hole drilling techniques [36], will be used to quantify residual stresses and to study their distribution. For example, in the layer-removal technique, by measuring the corresponding curvature after removing successive layers through the thickness, the initial distribution of residual stresses can be reconstructed.

8 Conclusions and future work

Hybrid manufacturing is now emerging as the next generation in manufacturing technologies where different operations are carried out on a single platform. This paper proposes a novel concept for hybrid manufacture, consisting of synergistically combining additive, subtractive and inspection processes. However, this combination of processes leads to new issues, namely part distortions and reduced part quality. A part is decomposed into a number of subparts that are built one by one. (i.e. one subpart is added onto another subpart that has already been manufactured). In this case, part distortions occur due to the residual stresses arising from the temperature difference between the new subpart being deposited (205 °C) and the previously made subpart (20 °C). This paper presents the first attempt at identifying and understanding part distortion behaviour in this hybrid manufacturing approach.

A robust experimental approach is used to identify and understand the distortion problem. The ANOVA results as shown in Table 3 indicate that the height of the existing part is of critical significance, followed by the section length. Thus, the interaction of these two factors is of primary

significance to part distortion. Long section length and thin existing part are detrimental to dimensional accuracy since a great degree of distortion was observed. For the existing part of 3mm in height and 120mm in length, the maximum accuracy deviation in height was 1.16mm when depositing new material onto it. In addition, the height of the newly deposited part and the layer thickness are insignificant, as indicated by the probability (*P*) of 0.16 and 0.56 in Table 3, respectively. However, interactions between height of the existing part and the newly deposited part or layer thickness contribute to the majority of changes in distortion deviation. The maximum change in distortion displacement (see Table 2) achieved was 1.17mm, when changing both existing part height and layer thickness. Moreover, it should be noted that most FFF parameters are interrelated and therefore cannot be considered to be independent factors to part distortion.

The underlying reason causing part distortion is the accumulation of residual stresses resulting from non-uniform temperature gradients in continuous heating and cooling cycles during the deposition process. Further efforts should be made to investigate the effects resulting from other FFF process parameters, such as deposition pattern, part geometry, porosity and deposition speed. Additionally, the interactions of layer thickness and other parameters (such as section length, existing part height, deposition pattern and speed) need further investigation. Therefore, there is a requirement to develop a robust model using a finite element analysis (FEA) technique, analysing the influence of the above factors. This FEA model should also be able to simulate 3D transient heat conduction and convection based on different deposition patterns and toolpaths, with the potential to reflect the real object in the deposition process. This will lead to the creation of a novel, rigorous and robust analytical method that can predict and determine distortion and part deviation issues. This research is critical to the continued understanding of combining disparate manufacturing processes for the emerging domain of hybrid manufacture.

References

[1] B. Lauwers, F. Klocke, A. Klink, A. E. Tekkaya, R. Neugebauer, and D. Mcintosh, "Hybrid processes in manufacturing," *CIRP Annals-Manufacturing Technology,* vol. 63, pp. 561-583, 2014.

[2] R. Kolleck, R. Vollmer, and R. Veit, "Investigation of a combined micro-forming and punching process for the realization of tight geometrical tolerances of conically formed hole patterns," *Cirp Annals-Manufacturing Technology,* vol. 60(2), pp. 331-334, 2011.

[3] Z. Zhu, V. Dhokia, A. Nassehi, and S. T. Newman, "A Review of Hybrid Manufacturing Processes - state of the art and future perspectives," *International Journal of Computer Integrated Manufacturing*, vol. 26, pp. 596-615, 2013.

[4] R. Ponche, O. Kerbrat, P. Mognol, and J.-Y. Hascoet, "A novel methodology of design for Additive Manufacturing applied to Additive Laser Manufacturing process," *Robotics and Computer-Integrated Manufacturing*, vol. 30, pp. 389-398, 2014.

[5] K. Karunakaran, S. Suryakumar, V. Pushpa, and S. Akula, "Low cost integration of additive and subtractive processes for hybrid layered manufacturing," *Robotics and Computer-Integrated Manufacturing*, vol. 26, pp. 490-499, 2010.

[6] S. Simhambhatla and K. Karunakaran, "Build strategies for rapid manufacturing of components of varying complexity," *Rapid Prototyping Journal*, vol. 21, pp. 340-350, 2015.

[7] J. H. Hur, J. Lee, h. Zhu, and J. Kim, "Hybrid rapid prototyping system using machining and deposition," *Computer-Aided Design*, vol. 34, pp. 741-754, Sep 2002.

[8] J. Ruan, K. Eiamsa-ard, and F. Liou, "Automatic process planning and toolpath generation of a multiaxis hybrid manufacturing system," *Journal of manufacturing processes*, vol. 7, pp. 57-68, 2005.

[9] J. Y. Jeng and M. C. Lin, "Mold fabrication and modification using hybrid processes of selective laser cladding and milling," *Journal of Materials Processing Technology*, vol. 110, pp. 98-103, Mar 2001.

[10] Y. A. Song and S. Park, "Experimental investigations into rapid prototyping of composites by novel hybrid deposition process," *Journal of Materials Processing Technology*, vol. 171, pp. 35-40, Jan 2006.

[11] K. Karunakaran, S. Suryakumar, V. Pushpa, and S. Akula, "Low cost integration of additive and subtractive processes for hybrid layered manufacturing," *Robotics and Computer-Integrated Manufacturing*, vol. 26 (2010), pp. 490-499, 2010.

[12] L. Ren, T. Sparks, J. Z. Ruan, and F. Liou, "Integrated Process Planning for a Multiaxis Hybrid Manufacturing System," *Journal of Manufacturing Science and Engineering-Transactions of the Asme*, vol. 132, Apr 2010.

[13] A. H. Nickel, D. M. Barnett, and F. B. Prinz, "Thermal stresses and deposition patterns in layered manufacturing," *Materials Science and Engineering a-Structural Materials Properties Microstructure and Processing*, vol. 317, pp. 59-64, Oct 2001.

[14] B. Wiedemann, K. H. Dusel, and J. Eschl, "Investigation into the influence of material and process on part distortion," *Rapid Prototyping Journal*, vol. 1, pp. 17-22, 1995.

[15] K. Dalgarno, T. Childs, I. Rowntree, and L. Rothwell, "Finite element analysis of curl development in the selective laser sintering process," in *Proceedings of Solid freeform fabrication symposium, University of Texas, Austin, TX*, 1996, pp. 559-566.

[16] F. O. Sonmez and H. T. Hahn, "Thermomechanical analysis of the laminated object manufacturing (LOM) process," *Rapid Prototyping Journal*, vol. 4, pp. 26-36, 1998.

[17] Y. W. Zhang and A. Faghri, "Melting of a subcooled mixed powder bed with constant heat flux heating," *International Journal of Heat and Mass Transfer*, vol. 42, pp. 775-788, Mar 1999.

[18] R. Chin, J. Beuth, and C. Amon, "Successive deposition of metals in solid freeform fabrication processes, Part 1: thermomechanical models of layers and droplet columns," *Journal of manufacturing science and engineering,* vol. 123, pp. 623-638, 2001.

[19] H. Xu, Y. Zhang, B. Lu, and D. Chen, "Numerical simulation of solidified deformation of resin parts in stereolithography rapid prototyping," *Jixie Gongcheng Xuebao(Chinese Journal of Mechanical Engineering)(China),* vol. 40, pp. 107-112, 2004.

[20] H. J. Yang, P. J. Hwang, and S. H. Lee, "A study on shrinkage compensation of the SLS process by using the Taguchi method," *International Journal of Machine Tools & Manufacture,* vol. 42, pp. 1203-1212, Sep 2002.

[21] N. W. Klingbeil, J. L. Beuth, R. K. Chin, and C. H. Amon, "Measurement and modeling of residual stress-induced warping in direct metal deposition processes," in *Solid Freeform Fabrication Proceedings, August, 1998*, H. L. Marcus, J. J. Beaman, D. L. Bourell, J. W. Barlow, and R. H. Crawford, Eds., ed Austin: Univ Texas Austin, 1998, pp. 367-374.

[22] A. Bellini and S. Guceri, "Mechanical characterization of parts fabricated using fused deposition modeling," *Rapid Prototyping Journal,* vol. 9, pp. 252-264, 2003.

[23] J. Yu, X. Lin, L. A. Ma, J. J. Wang, X. L. Fu, J. Chen, *et al.*, "Influence of laser deposition patterns on part distortion, interior quality and mechanical properties by laser solid forming (LSF)," *Materials Science and Engineering a-Structural Materials Properties Microstructure and Processing,* vol. 528, pp. 1094-1104, Jan 2011.

[24] T. M. Wang, J. T. Xi, and Y. Jin, "A model research for prototype warp deformation in the FDM process," *International Journal of Advanced Manufacturing Technology,* vol. 33, pp. 1087-1096, 2007.

[25] Y. Zhang and K. Chou, "A parametric study of part distortions in fused deposition modelling using three-dimensional finite element analysis," *Proceedings of the Institution of Mechanical Engineers Part B-Journal of Engineering Manufacture,* vol. 222, pp. 959-967, Aug 2008.

[26] J. S. S. Chen and H. Y. Feng, "Contour generation for layered manufacturing with reduced part distortion," *International Journal of Advanced Manufacturing Technology,* vol. 53, pp. 1103-1113, Apr 2011.

[27] M. Vatani, F. Barazandeh, A. Rahimi, and A. S. Nezhad, "Distortion modeling of SL parts by classical lamination theory," *Rapid Prototyping Journal,* vol. 18, pp. 188-193, 2012.

[28] Z. Zhu, V. Dhokia, and S. T. Newman, "Application of a hybrid process for high precision manufacture of difficult to machine prismatic parts," *International Journal of Advanced Manufacturing Technology,* vol. 74, pp. 1115-1132, 2014.

[29] Z. Zhu, V. Dhokia, and S. Newman, "A novel decision-making logic for hybrid manufacture of prismatic components based on existing parts," *Journal of Intelligent Manufacturing (in press),* 2014.

[30] Z. Zhu, V. G. Dhokia, and S. T. Newman, "The development of a novel process planning algorithm for an unconstrained hybrid manufacturing process," *Journal of Manufacturing Processes,* vol. 15, pp. 404-413, 2013.

[31] S. T. Newman, Z. Zhu, V. Dhokia, and A. Shokrani, "Process planning for additive and subtractive manufacturing technologies," *CIRP Annals - Manufacturing Technology (in press),* 2015.

[32] Q. Sun, G. Rizvi, V. Giuliani, C. Bellehumeur, and P. Gu, "Experimental study and modeling of bond formation between ABS filaments in the FDM process," in *ANTEC conference proceedings*, 2004, pp. 1158-1162.

[33] J. F. Rodriguez, J. P. Thomas, and J. E. Renaud, "Characterization of the mesostructure of fused-deposition acrylonitrile-butadiene-styrene materials," *Rapid Prototyping Journal*, vol. 6, pp. 175-185, 2000.

[34] A. K. Sood, R. K. Ohdar, and S. S. Mahapatra, "Improving dimensional accuracy of Fused Deposition Modelling processed part using grey Taguchi method," *Materials & Design,* vol. 30, pp. 4243-4252, Dec 2009.

[35] P. Withers and H. Bhadeshia, "Residual stress. Part 1–measurement techniques," *Materials science and Technology*, vol. 17, pp. 355-365, 2001.

[36] A. Turnbull, A. Maxwell, and S. Pillai, "Residual stress in polymers - evaluation of measurement techniques," *Journal of materials science*, vol. 34, pp. 451-459, 1999.